Indian Journal of Chemical Technology
Vol. 32, May 2025, pp. 395-406
DOI: 10.56042/ijct.v32i3.8911

Sequential sorption-photocatalytic method using polypyrrole@TiO_2 nanocomposites for the removal of agrochemicals

Pareshkumar G Moradeeya[1,2], Madhava Anil Kumar[3], Archana Sharma[1] & Shaik Basha[2]*

[1]Department of Environmental Science & Engineering, Marwadi University, Rajkot-360 003, Gujarat, India

[2]Hyderabad Zonal Centre, CSIR-National Environmental Engineering Research Institute, IICT Campus, Tarnaka, Hyderabad-500 007, Telangana, India

[3]Centre for Rural and Entrepreneurship Development, National Institute of Technical Teachers Training and Research, Chennai-600 113, India

*E-mail: s_basha@neeri.res.in

Received 19 February 2024; accepted 20 March 2025

The sequential batch process for the degradation of selected agrochemicals 2,4-dichlorophenoxyacetic acid (2,4-D) and triclopyr acid (TCP) using the synergistic effect of a fabricated photocatalyst are performed. The photocatalysts have been fabricated by doping titanium dioxide with polypyrrole (PP-TiO_2) and tested for its adsorption-photocatalysis property to remove the hazardous agrochemicals. Subsequent characterization tools are used to understand morphology and other features of the catalysts. Batch sorption-photocatalysis are performed to assess the performance of the fabricated photocatalysts against 2,4-D and TCP. The outcome of sequential experiments evaluated the equilibrium and kinetic profile that includes rate constants and efficiencies. The mechanism adopted by PP-TiO_2 is found through interactions and electrostatic attractions that facilitated better removal of herbicides. The selected herbicides are effectively degraded by utilizing a newer design for a scale-up procedure that used a recirculating semi-batch reactor. The experimental versus predicted values of the reactions were evaluated and it was found in agreement among the values. The presented research would be first to discuss the induction of a semi-batch reactor for the fabrication of nanocomposites and degradation of agrochemicals using a sequential adsorption-photocatalytic technique.

Keywords: Adsorption, Agrochemicals, Chemical polymerization, Degradation, Photocatalysis, Polypyrrole

Introduction

The massive influence of natural and anthropogenic organic chemicals discharged into the environment necessitates a deeper understanding of these chemicals to the environment. Several harmful organic compounds have been detected in water[1,2,3]. The toxicity of these substances, their resistance to natural decomposition, and their propensity to survive in the environment have been the source of significant concern for societies and regulatory bodies all over the world[4]. These organic pollutants are poisonous, persistent, tend to bio-accumulate, and can be classified as hazardous substances under existing legislation[5,6]. These compounds infiltrate water bodies after being used or improperly disposed and may be transferred to the soil, water sources, and groundwater, leaving extensive residues in the ecosystem[6,7,8]. Ecosystem contamination with persistent chemicals has direct or indirect impacts on fauna, flora, and human health[9,10].

Advanced oxidation techniques are used to treat structurally distinct pollutants and mineralize them into simpler products through a series of chemical reactions rather than merely going through a phase change[11]. Photocatalysis is a cost-effective oxidative technique for converting diverse environmental pollutants[12,13,14,15]. TiO_2 (titanium dioxide) is widely utilized photo-catalyst which insoluble but easily dispersed in water. However, recovery of TiO_2 from the aqueous media remains to be a constraint. The issue of photocatalyst separation from the processing fluid is solved by the binding of TiO_2 particles to certain surfaces[16]. Photocatalysis and adsorption have a synergistic effect on pollutant breakdown in water[17, 18, 19, 20].

Conductive polymers possess a combination of mechanical, chemical, and physical properties, which are enhanced by their electrical and photocatalytic features seen in semiconductors materials[21,22]. Polypyrrole (PP)-TiO_2 is a composite material consisting of a reticulate doped polymer and titanium dioxide. It possesses distinctive characteristics that facilitate the generation of charge transfer inside an

uninterrupted conductive system in the reticulate treated polymer, resulting in high conductivity[22, 23]. PP-TiO_2 composites are synthesized by distinct methods such as polymerization, surface molecular imprinting, and micro-emulsion in presence of precursors, solvents, photosensitizer and oxidants[22, 24].

The chemical polymerization has several advantages that includes low cost, ease of processing, improved solid stability, structural crystallinity, higher productivity and lower environmental effect[21,25,26]. The applicability of the PP-TiO_2 nanocomposites were reported for the remediation of methyl orange, methylene blue, rhodamine B, diclofenac, 4-chlorophenol, polyethylene and nitrate from water[24,27-31]. However, the degradation of persistent organics are not easier when compared to the dye molecules, hence efficacy of these photocatalysts for dye degradation do not provide a roadmap for the degradation of persistent organics. Thus, the present research is aimed to study the applicability of polypyrrole as a support for TiO_2 and to aid adsorptive removal for further facilitation of photocatalytic removal of the contaminants. To understand the functional behaviour of the synthesized materials which helps in the removal of selected herbicides and fabricate a semi-batch reactor. Concomitantly, to investigate the kinetic profile and equilibria of 2,4-Dichlorophenoxyacetic acid (2,4-D) and Triclopyr acid (TCP) removal by the nanocomposites as well as to evaluate the reusability of the used PP-TiO_2.

Experimental Section

Chemicals

The stock solutions of 2,4-D (Otto Chemical Company) and TCP (Aimco Pesticides) were produced in a solvent system of methanol and water at a concentration of 2.5 g/L of both herbicides separately. These solutions were then diluted with distilled water, following the HPLC conditions described in a previous work[32]. Pyrrole (Sigma Aldrich), $FeCl_3$ supplied by Fisher Scientific while HCl & NaOH from Qualigens, Acetonitrile (HPLC Grade), were used.

Synthesis of nanocomposites

The synthesis of PP-TiO_2 nanocomposites were carried out by a method described by Chen *et al*.[33], with slight modifications. For this purpose, a varying amount of TiO_2 was mixed with 100 mL of acidic water in an ultrasound water-bath for 15 min followed by the addition of 0.167 mL of pyrrole. Ferric chloride solution (0.811 g/10 mL in acidic water) was added dropwise. The beaker was moved to a cold environment for the remainder of the overnight (24 h), and the blackish was cleaned by washing it with deionized water, organic solvent (MeOH), and acidic water. Subsequently, more distilled water was added until the water coming out of the filter was clear. This pure and polypyrrole composite dried for 24 h at 60°C. When creating the composite material, different amounts of TiO_2 (0.798, 1.597, and 2.395 g) were used, and the materials were labeled as PP-$TiO_{2(a)}$, PP-$TiO_{2(b)}$ and PP-$TiO_{2(c)}$, respectively. The above-mentioned acidic water was 1.0 N HCl.

Characterization of synthesized nanocomposites

Field emission scanning electron microscopy (FE-SEM) was employed to examine the surface characteristics of produced composites at high magnifications. X-ray diffraction patterns were acquired using a Philips X'Pert system with Cu-Kα radiation. The FT-IR spectra were obtained using a Shimadzu FT-IR spectroscopy instrument (FTIR-8400S) at room temperature, with a KBr beam splitter of FTIR grade. UV-visible absorption was performed using a UV/visible spectrometer manufactured by PG Instrument from the United Kingdom.

Batch experimental design

Under the influence of ultraviolet light emanating from a 125-W high-pressure mercury lamp, the photocatalytic activity of composite (polypyrrole/ TiO_2) was investigated for its ability to degrade selected herbicide at 365 nm light. Experiments involving adsorption and photochemistry were carried out in a photocatalytic apparatus, continual stirring, and water cooling. In order to establish the contribution of adsorption to the total removal rate of herbicides, adsorption performed in dark for a period of 30 min before the photodegradation process was carried out. After the adsorption equilibrium was reached, the pesticide solutions that contained catalyst composites were next photo-catalytically degraded by exposing them to ultraviolet light. In the screening experiments, a constant amount of catalyst load and herbicide concentration was utilized. After obtaining an aliquot of 1.0 mL at a number of different time periods and filtering it, the photocatalyst was composited and separated (0.22 m nylon syringe filters). The choice of photocatalyst was made based on the equation given below.

$$Removal\ (\%) = \left(\frac{C_i - C_f}{C_i}\right) \times 100 \quad ...(1)$$

where C_f and C_i are the final and initial concentration of 2,4-D and TCP at time. The adsorption and kinetics experiments performed with various concentration of 2,4-D and TCP by the synthesized PP-TiO_2 is calculated by;

$$q_e = \left(\frac{C_i - C_e}{m}\right) v \quad ...(2)$$

where C_e is concentration of 2,4-D and TCP at equilibrium; V is volume (L) and W is weight (g) of PP-TiO_2.

Results and Discussion

Screening of PP-TiO_2 for herbicides degradation

The properties of the three synthesised nanocomposites were distinguished from TiO_2 with respect to 2,4-D and TCP removal through photocatalysis followed by adsorption. For this purpose, 0.5 g/L of the fabricated materials and TiO_2 were screened individually with 10 mg/L of each pesticide for initial adsorption of 30 min followed by photocatalysis for an additional time of 120 min. Results are depicted in Fig. 1 and observed that under UV light, photocatalytic degradation of 2,4-D and TCP occurred at its best by all PP-TiO_2 when compared to pristine TiO_2. In order of greater success rates, the removal activity of PP-TiO_2 composites was sorted as follows: PP-$TiO_{2(a)}$> PP-$TiO_{2(b)}$> PP-$TiO_{2(c)}$> TiO_2. Therefore, PP-$TiO_{2(a)}$ was used for further investigation and is evident that the activities of PP-$TiO_{2(a)}$ nanocomposites were higher than pristine TiO_2 after adsorption and photocatalysis; comparable results were discovered in an earlier experiment[32]. Because of the presence of methanol in the reaction mixture, the removal of 2,4-D and TCP by TiO_2 through photocatalysis was significantly lower[34,35]. The above phenomena demonstrate zippo adsorption for 2,4-D and TCP after establishing the adsorption equilibrium, revealing the declined photocatalytic efficacy of pure TiO_2. After 30 min, the reaction sets showed effective adsorption, which is consistent with the results that demonstrated the superiority of the nanocomposite over the bare TiO_2. Improved photo-response of PP-$TiO_{2(a)}$ nanocomposite is due to the surface modification of TiO_2 with polypyrrole.

Characterization of the prepared nanocomposite

FT-IR analyses

Fig. S1 (Supplementary information) shows the IR spectra with usual peaks of undoped TiO_2 and PP-TiO_2. FT-IR spectrum of TiO_2 exhibited only three significant absorption peaks between 3419 and 1637 cm^{-1} due to OH stretching vibrations[33,36]. Ti-O-Ti stretching vibration is connected with the observed strong band at 609 cm^{-1}, indicating the development of anatase TiO_2[32,37]. The IR spectrum of PP-TiO_2 shows the C=O at 2336 cm^{-1} for the carbon dioxide adsorption by the composites. C=C and C-C in the pyrrole ring are represented by peaks at 1544 and 1456 cm^{-1}, respectively[27,38]. C-N stretch and C-H deformation of polypyrrole were allocated to the bands 1178 and 1030 cm^{-1}(Ref. 27, 38).

X-ray diffraction analyses

Fig. S2 demonstrates that anatase TiO_2 appears crystalline by displaying the diffraction patterns of both native TiO_2 and polypyrrole coated TiO_2[33,39]. The major peaks are found at the crystal planes; (101), (004), (200), (105), (211), and (204) which was in agreement with JCPD standards (No. 21-1272) of tetragonal anatase[32,40]. XRD pattern of PP-TiO_2 revealed that at the equivalent site of pure TiO_2 in

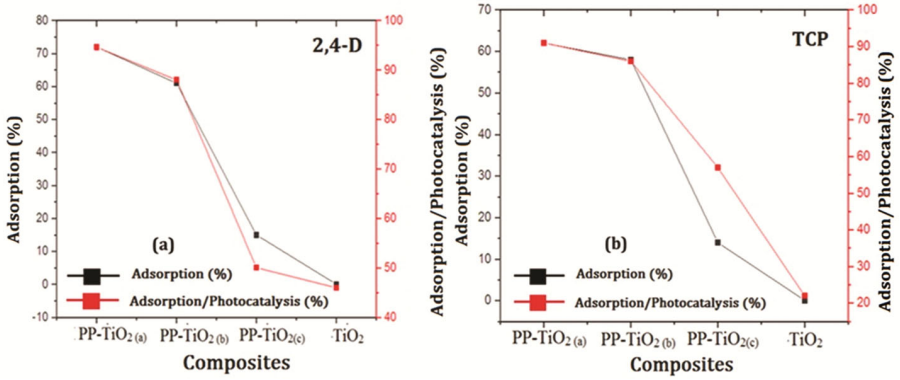

Fig. 1 — Assortment of nanocomposite for test (a) 2,4-D and (b) TCP (C_o: 10 mg/L; T: 298 K; t: 120 min; I: 10 W/m^2; PP-TiO_2: 0.5 g/L)

polypyrrole matrix, almost the same strong diffraction peaks exist. Coating of polypyrrole onto TiO_2 did not modify its crystallinity. At the same time, the pattern of the PP-TiO_2 composites did not acquire any extra diffraction peaks, which may be because there was only a little amount of polypyrrole present in the composites[27,38]. However, the diffraction peak intensity slightly decreased, which could be due to the presence of polypyrrole coating.

UV-visible spectrophotometric analyses

Absorption spectra of pure TiO_2 and PP-TiO_2 (Fig. S3) exhibited significant absorption in the visible area and peak in the ultraviolet (UV) region. Photo-generation by TiO_2 is connected to the strong signal centered in the UV zone where a prominent peak was observed near the visible zone in the spectrum of PP-$TiO_{2(a)}$ nanocomposite, which is associated to the $\pi \rightarrow \pi^*$ electronic transitions of delocalized pi-bonds[41]. The absorption peak of PP-$TiO_{2(a)}$ exerts a red shift, representing that the material showed good efficiency towards degradation of targeted pollutants under different light sources (i.e. UV, visible and sun light)[22,42]. Estimated band gap energies were 3.2 and 2.4 eV for pure TiO_2 and PP-TiO_2, respectively, from Tauc's plot (Fig. S4). As a result, PP-TiO_2 nanocomposites formed substantially more electron-hole pairs than untainted TiO_2 when excited by UV radiation leading to greater photocatalysis[27].

Electron microscopic analyses

Fig. S5 displays the surface morphology of TiO_2 and PP-$TiO_{2(a)}$ at different magnifications. The nano-grains of TiO_2 particles are of uniform size and appear agglomerated[32]. The high surface area of the composite led to a rise in the surface properties of the material, which in turn led to a greater extent of light absorption. Consistent dispersal of polypyrrole across TiO_2 can be noticed and infers the PP-TiO_2 composite is built up of granular complexes[32]. The efficacy of PP-TiO_2 in terms of either adsorption or photocatalysis is significantly improved owing to the unstructured and granular nature of the material, which results in an overall roughness.

Adsorption isotherm and kinetics study

Isotherm evaluation were used to investigate the distribution of 2,4-D and TCP molecules at PP-$TiO_{2(a)}$'s surface during adsorption. Four distinct models were used to examine the equilibrium *viz.,* Langmuir, Freundlich, Sips and Redlich-Peterson (RP) isotherms[32,43,44]. Fig. 2 illustrates the non-linear trend of these isotherms with various critical parameters in fitting the experimental data during 2,4-D and TCP removal. Table 1 provides the correlation coefficients (R^2) and other statistical information of adsorption by PP-$TO_{2(a)}$. For the tested concentrations of 2,4-D and TCP; isotherm expressed a high R^2 value of 0.999 and RSS value revealed significance between C_e and q_e[45]. The adequacy of R-P isotherm confirms the sorption of 2,4-D and TCP onto surface of PP-$TiO_{2(a)}$.

Another key aspect that determines the sorption efficiency is the adsorption kinetics and to understand the removal mechanism with respect to time, four different kinetic models were used[44,46-49]. The optimal model was chosen based on non-linear R^2 and RSS as well as the calculated q_e values as given in the Tables 2 & 3. Pseudo-second order data had good fit (R^2, 0.999-1) with minimum error for both pesticides, when compared with the pseudo-first order and other kinetic models. Pseudo-second order model predominates the elimination of agrochemicals at

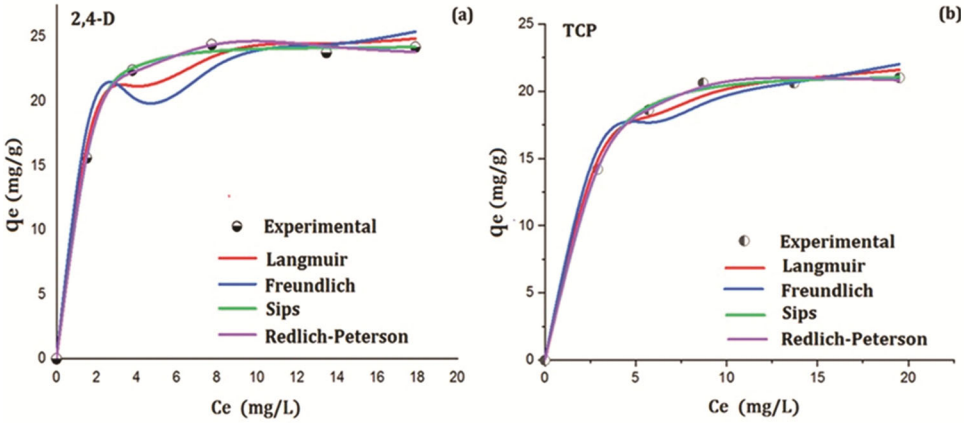

Fig. 2 — Adsorption isotherm curves of (a) 2,4-D and (b) TCP removal (t: 30 min; T: 298 K; PP-TiO_2: 0.5 g/L)

Table 1 — Equilibrium isotherm constants for 2,4-D and TCP removal by PP-TiO_2

Parameters	Isotherms	2,4-D	TCP
	Langmuir		
Q_{max} (mg/g)	$q_e = \frac{Q_{max} K_L C_e}{1 + K_L C_e}$	26.085	23.442
K_L (L/mg)		1.143	0.594
R_L	$R_L = \frac{1}{1 + K_L C_0}$	0.153	0.189
Reduced χ^2		1.039	0.495
R^2 (COD)		0.990	0.994
Adj. R^2		0.988	0.992
RSS		4.158	1.983
	Freundlich		
K_F (L/mg)		16.792	12.956
n		6.966	5.611
Reduced χ^2	$q_e = K_F C_e^{\frac{1}{n}}$	3.633	1.602
R^2 (COD)		0.968	0.980
Adj. R^2		0.960	0.975
RSS		14.533	6.408
	Redlich-Peterson		
K_{RP} (L/mg)		17.424	8.062
a_{RP}(L/mg)		0.414	0.175
β		1.169	1.217
Reduced χ^2	$q_e = \frac{K_{RP} C_e}{1 + a_{RP} C_e^{\beta}}$	0.139	0.088
R^2 (COD)		0.999	0.999
Adj. R^2		0.998	0.998
RSS		0.419	0.265
	Sips		
Q_{max}(mg/g)		24.269	21.251
B (L/mg)		0.873	0.485
n		2.160	2.021
Reduced χ^2	$q_e = \frac{Q_{max} B C_e^n}{1 + B C_e^n}$	0.142	0.099
R^2 (COD)		0.999	0.999
Adj. R^2		0.998	0.998
RSS		0.426	0.298

lower concentrations and the smaller particle size drives the inclusive adsorption[45]. High R^2 and low RSS values confirm that the pseudo-second-order kinetics describe the sorption of the targeted pollutants by PP-$TiO_{2(a)}$.

Effect of reaction pH on photodegradation

Photodegradation is influenced by solution pH which was examined using fixed concentration of pesticides (2,4-D, 20 mg/L and TCP, 10 mg/L) and 0.5 g/L PP-$TiO_{2(a)}$. The reaction sets maintained at various levels of pH 4-10 and were exposed to light for 120 min. The adsorption and photocatalytic performance of PP-$TiO_{2(a)}$ decreased with the increase in the solution pH, the highest efficiency for 2,4-D removal was observed at pH 5 while pH 4 for TCP removal as shown in Fig. 3. Polypyrrole is known to deprotonate under alkaline circumstances and NH group in their matrix attracts anions electrostatically, thereby reducing the photocatalytic efficiency at elevated pH levels[50-54]. The low pH was more favourable for selected herbicides, PP-$TiO_{2(a)}$ adsorbed 58% of 2, 4-D at pH 5 and 62, % of TCP at pH 4, respectively at 30 min.

Effect of initial 2,4-D and TCP concentration on photo-degradation

The influence of initial 2,4-D and TCP concentration on photodegradation by PP-$TiO_{2(a)}$ was studied through various concentrations individually for 2 h. Photocatalytic degradation decreased with the rise in initial concentration (C_i) of 2,4-D and TCP as shown in Figs 4(a) & 5(a), and this is due to non-availability of active sites on PP-$TiO_{2(a)}$'s surface[55]. Previously mentioned condition made only few photons to reach the PP-$TiO_{2(a)}$'s surface, thus reducing the generation of hydroxyl radicals[55,56].

Modelling of photocatalytic activity

Based on assumption that the rate of pesticide degradation is directly proportional to the photocatalyst dose (C_{PC}) and inversely proportional to initial pesticide concentration (C_i) in a recirculating photocatalytic

Table 2 — Estimated kinetic values of 2,4-D and TCP removal by PP-TiO_2

Parameters	Equations	2,4-D				TCP			
		10 mg/L	15 mg/L	20 mg/L	25 mg/L	10 mg/L	15 mg/L	20 mg/L	25 mg/L
Pseudo-first order									
q_e(mg/g)	$qt = q_e(1-e^{-kt})$	12.951	20.443	24.399	25.828	11.958	16.046	18.452	21.596
k_1 (1/min)		0.304	0.326	0.357	0.344	0.302	0.342	0.382	0.410
Reduced χ^2		0.080	0.262	0.346	0.338	0.106	0.100	0.175	0.132
R^2 (COD)		0.998	0.997	0.997	0.997	0.996	0.998	0.997	0.998
Adj. R^2		0.997	0.996	0.996	0.997	0.995	0.997	0.997	0.998
RSS		0.241	0.786	1.039	1.016	0.107	0.100	0.175	0.132
Pseudo-second order									
q_e(mg/g)	$qt = \frac{k_2 q_e^2 t}{1 + k_2 q_e t}$	14.039	22.008	26.017	27.637	12.992	17.169	19.547	22.674
k_2 (g/mg/min)		0.039	0.028	0.028	0.025	0.041	0.040	0.044	0.045
h (mg/g/min)		7.686	13.561	18.952	19.095	6.920	11.790	16.811	23.134
Reduced χ^2		0.002	$5x10^{-4}$	0.002	$1.57x10^{-4}$	$5.45x10^{-4}$	0.003	0.001	0.019
R^2 (COD)		0.999	1	0.999	1	0.999	0.999	0.999	0.999
Adj. R^2	$h = k_2 q_e^2$	0.999	0.999	0.999	1	0.999	0.999	0.999	0.999
RSS		0.002	$5 x10^{-4}$	0.002	$1.57x10^{-4}$	0.002	0.010	0.006	0.059

Table 3 — Elovich and intraparticle diffusion kinetic values of 2,4-D and TCP removal by PP-TiO_2

Parameters	Equations	2,4-D				TCP			
		10 mg/L	15 mg/L	20 mg/L	25 mg/L	10 mg/L	15 mg/L	20 mg/L	25 mg/L
Elovich									
α (mg/g/min)	$qt = \frac{1}{\beta}\ln(\alpha\beta t)$	211.263	651.413	2523.715	1652.437	164.068	1019.421	5492.652	42063.763
B (g/mg)		0.615	0.426	0.410	0.367	0.650	0.591	0.604	0.611
Reduced χ^2		0.071	0.098	0.097	0.167	0.034	0.088	0.044	0.135
R^2 (COD)		0.998	0.999	0.999	0.998	0.999	0.998	0.999	0.998
Adj. R^2		0.997	0.998	0.999	0.998	0.998	0.998	0.999	0.998
RSS		0.213	0.295	0.293	0.501	0.102	0.264	0.134	0.407
Intraparticle diffusion									
k_{id} (mg/g/$min^{0.5}$)	$qt = k_{id}\sqrt{t} + C_i$	2.370	3.732	4.430	4.696	2.195	2.914	3.335	3.867
C		2.394	3.939	4.969	5.157	2.179	3.204	3.896	4.781
Reduced χ^2		7.170	19.217	30.412	32.881	5.903	12.730	18.655	28.158
R^2 (COD)		0.823	0.812	0.793	0.799	0.829	0.799	0.780	0.760
Adj. R^2		0.765	0.749	0.725	0.733	0.772	0.732	0.707	0.680
RSS		21.512	57.651	91.236	98.643	17.710	38.192	55.966	84.474

reactor (operated in batch mode) at constant temperature and light intensity. Photocatalytic activity of PP-$TiO_{2(a)}$ was modeled as a function of C_i and C_{PC} at constant temperature and light intensity for 2,4-D and TCP removal[57,58] as per the following equations.

$$k_{app-2,4-D} = k'_{2,4-D}\left(\frac{K_{R-2,4-D}}{1+K_{R-2,4-D}C_i}\right)(0.836)\left(\frac{K_{PC}C_{PC}}{1+K_{PC}C_{PC}}\right) \quad ...(3)$$

$$k_{app-TCP} = k'_{TCP}\left(\frac{K_{R-TCP}}{1+K_{R-TCP}C_i}\right)(1.479)\left(\frac{K_{PC}C_{PC}}{1+K_{PC}C_{PC}}\right) \quad ...(4)$$

where k_{app}: reaction rate constant (1/min); k_0: constant (mg/L); K_R: adsorption equilibrium constant (L/mg); C_i: initial pesticide concentration (mg/L); K_{PC}: sorption coefficient for PP-$TiO_{2(a)}$ dose (L/mg); C_{PC}: PP-$TiO_{2(a)}$ dose (mg/L).

Effect of initial pesticide concentration (C_i)

Degradation kinetics of 2,4-D and TCP follows pseudo-first order kinetics as per Eq. (5);

$$r_{2,4-D\ or\ TCP} = -\left(\frac{dC_f}{dt}\right) = k_1 C_f \quad ...(5)$$

Photocatalysis follow Langmuir-Hinshelwood (L-H) model, as shown in Eq. (6);

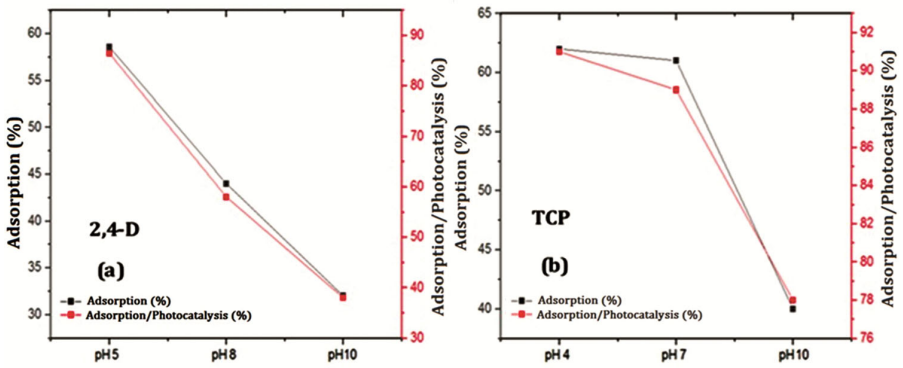

Fig. 3 — Effect of pH on photocatalysis - adsorption (a) 2,4-D (b) TCP (*t*: 150 min; T: 298 K; PP-TiO_2: 0.5 g/L)

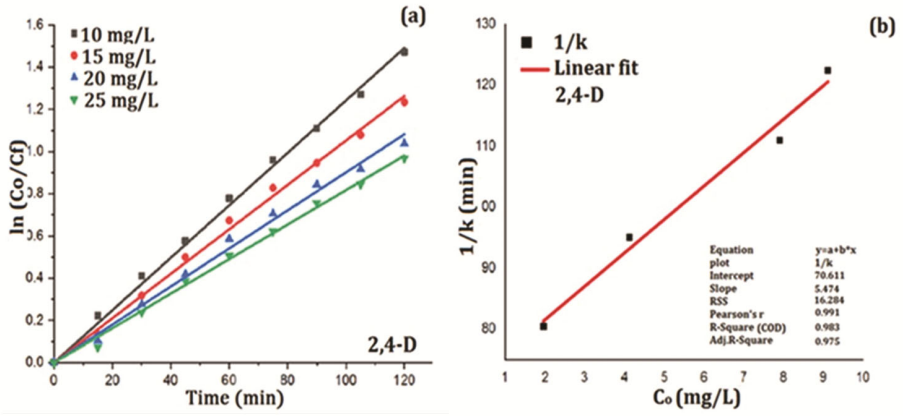

Fig. 4 — (a) Influence of the initial concentration of 2,4-D and (b) modified L-H. (I: 10 W/m^2; PP-TiO_2: 0.5 g/L; T: 298 K)

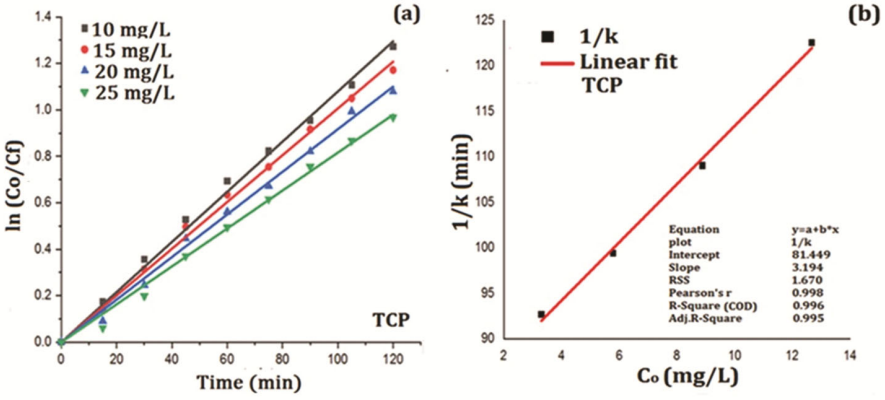

Fig. 5 — (a) Influence of the initial concentration of TCP and (b) modified L-H. (I: 10 W/m^2; PP-TiO_2: 0.5 g/L; T: 298 K)

$$r_{2,4-D\ or\ TCP} = \frac{K_{LH}K_R C_f}{1+K_R C_i} \quad ...(6)$$

Substituting the values of $r_{2,4\text{-}D\ or\ TCP}$ from Eq. (5) into Eq. (6) to arrive at Eq. (7):

$$r_{2,4-D\ or\ TCP} = \frac{K_{LH}K_R C_f}{1+K_R C_i} = k_1 C_f \quad ...(7)$$

$$k_1 = \frac{K_{LH}K_R}{1+K_R C_i} \quad ...(8)$$

where k_1: rate constant (1/min); $r_{2,4\text{-}D\ or\ TCP}$: reaction rate of 2,4-D or TCP (mg/L min); K_{LH}: reaction rate (mg/L min); t: time (min); K_R: equilibrium constant (L/mg); C_i: initial 2,4-D/TCP concentration (mg/L); C_f: final 2,4-D/TCP concentration (mg/L).

Table 4 — Rate constants for the photocatalytic degradation of 2,4-D and TCP by PP-TiO_2

	Effect of concentration for 2,4-D			
Parameter	10 mg/L	15 mg/L	20 mg/L	25 mg/L
k_{app}(1/min)	0.012	0.010	0.007	0.005
RSS	0.006	0.003	0.008	0.004
Pearson's r	0.999	0.999	0.998	0.999
R^2 (COD)	0.999	0.998	0.997	0.998
Adj. R^2	0.998	0.998	0.997	0.998
k_{LH} (mg/L/min)		0.183		
K_R (L/mg)		0.077		
	Effect of concentration for TCP			
	10 mg/L	15 mg/L	20 mg/L	25 mg/L
k_{app}(1/min)	0.011	0.010	0.009	0.008
RSS	0.006	0.004	0.005	0.006
Pearson's r	0.998	0.999	0.999	0.998
R^2 (COD)	0.998	0.999	0.998	0.997
Adj. R^2	0.998	0.998	0.998	0.997
k_{LH} (mg/L/ min)		0.313		
K_R (L/mg)		0.039		
	Effect of dosage for 2,4-D			
	0.25 g/L	0.5 g/L	1.0 g/L	-
k_{app}(1/min)	0.006	0.009	0.014	-
RSS	0.004	0.008	0.007	-
Pearson's r	0.998	0.998	0.999	-
R^2 (COD)	0.997	0.997	0.999	-
Adj. R^2	0.997	0.997	0.999	-
k_{LH}(mg/L/min)		0.122		
K_R (L/mg)		0.163		
	Effect of dosage for TCP			
	0.25 g/L	0.5 g/L	1.0 g/L	1.5 g/L
k_{app}(1/min)	0.007	0.011	0.014	0.018
RSS	0.002	0.007	0.029	0.078
Pearson's r	0.999	0.999	0.998	0.997
R^2 (COD)	0.999	0.998	0.996	0.994
Adj. R^2	0.999	0.998	0.996	0.994
k_{LH}(mg/L/min)		0.049		
K_R(L/mg)		0.074		

Photocatalytic degradation decreased with the rise in initial concentration (C_i) of 2,4-D and TCP as shown in Figs 4(a) & 5(a). Figs 4(b) and 5(b) illustrate the L-H model for 2,4-D and TCP, respectively. A correlation between k_1 and C_i from the modified L-H model is derived by transforming Eq. (8);

$$\frac{1}{k_1} = \frac{1}{K_{LH}} C_i + \frac{1}{K_{LH} K_R} \quad ...(9)$$

The kinetic constants (K_{LH} and K_R) for the pesticides tested are listed in Table 4.

Effect of catalyst dose (C_{PC})

$$k_4 = \frac{k_0 K_{PC} C_{PC}}{1 + K_{PC} C_{PC}} \quad ...(10)$$

where k_4: first-order rate constant for C_{PC} (1/min); k_0: reaction rate constant for C_{PC} (1/min); K_{PC}: adsorption constant for C_{PC} (L/mg); C_{PC}: PP-$TiO_{2(a)}$ dose (mg/L). Correlation between k_4 and C_{PC} can be established from the modified L-H model (from Eq.10);

$$\frac{1}{k_4} = \frac{1}{k_0 K_{PC}} \left(\frac{1}{C_{PC}}\right) + \frac{1}{k_0} \quad ...(11)$$

Photocatalytic degradation enhanced with the increasing quantity of catalyst, as illustrated in Figs 6(a) and 7(a) for 2,4-D and TCP, respectively. Figs 6(b) and 7(b) illustrate the L-H model for 2,4-D and TCP, respectively.

Model equation verification

The parameters such as K_R and K_{PC} were evaluated using non-linear regression analysis for both herbicides as mentioned in Table S1 (Supplementary

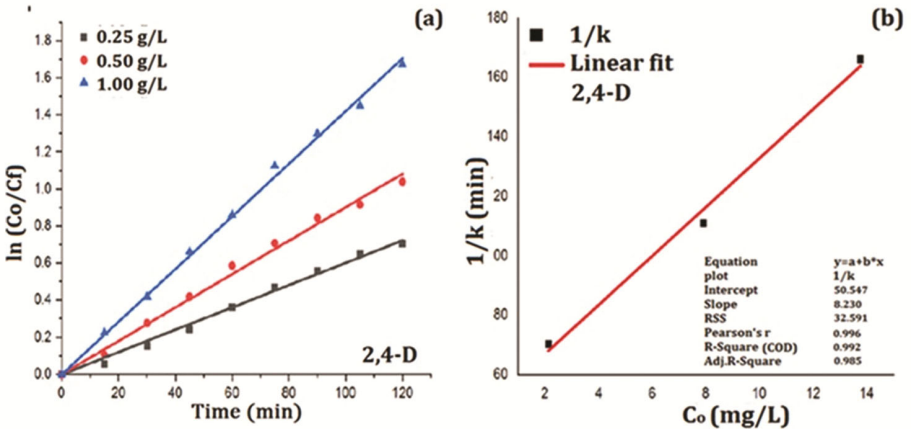

Fig. 6 — (a) Influence of PP-TiO_2 dose (b) L-H plot for 2,4-D photodegradation (C_i: 20 mg/L; pH: 5; T: 298 K; I: 10 W/m^2)

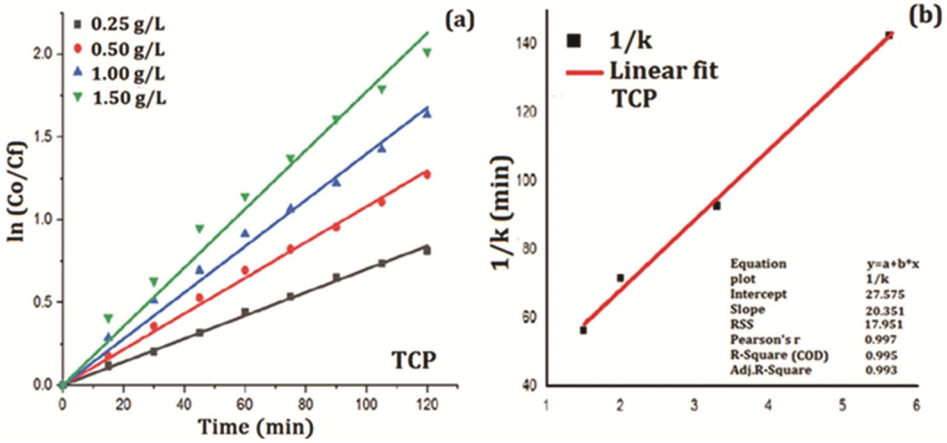

Fig. 7 — (a) Influence of PP-TiO_2 dose (b) L-H plot for TCP photodegradation (C_i: 10 mg/L, pH: 4; T: 298 K; I: 10 W/m^2)

Information). Using C_i and C_{PC}, the apparent rate constant (k_{app}) for 2,4-D and TCP were calculated[57]. Eqn. (12 & 13) are derived by substituting the values of Table S1 in the Eqs (12 & 13);

$$k_{app\ (2,4-D)} = 0.183\left(\frac{0.077}{1+0.077C_i}\right)0.836\left(\frac{0.122C_{PC}}{1+0.122C_{PC}}\right) \quad ...(12)$$

$$k_{app\ (TCP)} = 0.313\left(\frac{0.039}{1+0.039C_i}\right)1.479\left(\frac{0.049C_{PC}}{1+0.049C_{PC}}\right) \quad ...(13)$$

The experimental and predicted *kapp*of both the herbicides at different operational conditions (C_i and C_{TiO2}) was juxtaposed to evaluate the model as shown in Fig. 8. Very good correlation (R^2) was obtained between the experimental and model estimated data for both the herbicides as given in the Table S1.

Regeneration of photocatalyst

The practical feasibility and cost-effectiveness of a treatment approach depend on the ability to reuse the adsorbent/catalyst. In this study, the reusability of PP-$TiO_{2(a)}$ was tested by performing three photo-degradation cycles in a row under optimal conditions. PP-$TiO_{2(a)}$ was washed with water and organic solvent, 1 N HCL and distilled water before being rinsed after each cycle. After that, the recovered PP-$TiO_{2\ (a)}$ was dried (60°C) before being employed in the next cycle with freshly prepared solution.[32,59] After three successive cycles, the photo-degradation effectiveness of PP-TiO_2 deteriorated from 95.22 to 89% during 2,4-D removal while the removal was 91-86% in case of TCP removal (Supplementary Information, Fig. S6). The outcome of the reusability test shows that PP-$TiO_{2(a)}$ material considerable repeatability, with a minor decrease in photocatalytic activity subsequently 3 cycles of processes, This phenomenon might be ascribed to the agglomeration of particles during the catalytic process or the loss of catalyst during the recovery phase.[60, 61]

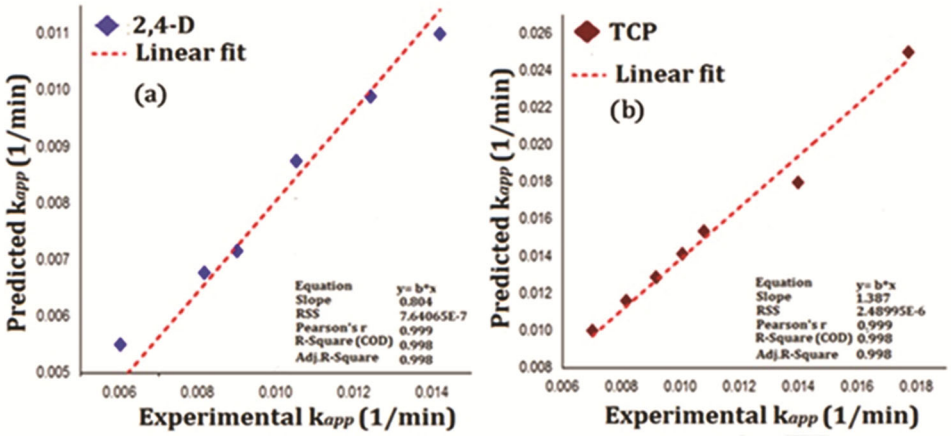

Fig. 8 — Juxtaposition of k_{app} values

Conclusion

A sequential adsorption followed by photo-degradation of two dreadful pesticides; 2,4-D and TCP from waster using PP-TiO_2 nanocomposites were achieved. The loading of polypyrrole onto TiO_2 created a significant impact on their pesticide removal efficiencies. The outcome of this work reveals that the fabricated PP-TiO_2 nanocomposites possessed high adsorption capacity that facilitated the photodegradation. Redlich-Peterson model reflected the experimental isotherm data, whereas pseudo-second order kinetics explained the sorption kinetics. PP-$TiO_{2(a)}$ had the highest k_{app} which allowed the enhanced removal of 2,4-D and TCP within 120 min. The reusability assays reveal that PP-TiO_2 retained 85% photocatalytic activity even after 3 cycles. Therefore, the PP-TiO_2 strongly justifies its candidature in removing dreadful pesticides from water environment.

Acknowledgement

The authors would like to extend their heartfelt gratitude to the Director of CSIR-NEERI, the Director of CSIR-CSMCRI, and the Management of Marwadi University for their invaluable support. The manuscript has been assigned the reference number CSIR-NEERI/KRC/2022/MARCH/HZC/1.

Supplementary Information

Supplementary information is available on the website http://nopr.niscpr.res.in/handle/123456789.

References

1 Tang F H M, Lenzen M, McBratney A & Maggi F, Risk of pesticide pollution at the global scale, *Nat Geosci*, 14 (2021) 206.

2 de-Souza R M, Seibert D, Quesada H B, de Jesus B F, Fagundes-Klen M R & Bergamasco R, Occurrence, impacts and general aspects of pesticides in surface water: A review, *Process Saf Environ Prot*, 135 (2020) 22.

3 Hasan M A, Ahmad S & Mohammed T, Groundwater contamination by hazardous wastes Arab, *J Sci Eng*, 46 (2021) 4191.

4 Qamar M, Muneer M & Bahnemann D, Heterogeneous photocatalysed degradation of two selected pesticide derivatives, triclopyr and daminozid in aqueous suspensions of titanium dioxide, *J Environ Manage*, 80 (2006) 99.

5 Bian X, Chen J & Ji R, Degradation of 2,4-dichlorophenoxyacetic acid (2, 4-D) by novel photocatalytic material of tourmaline-coated TiO_2 nanoparticles: Kinetic study and model, *Materials*, 6 (2013) 1530.

6 Dórea J G, Persistent, bioaccumulative and toxic substances in fish: human health considerations, *Sci Total Environ*, 400 (2008) 93.

7 Dehkordi M M, Nodeh Z P, Dehkordi K S, Khorjestan R R, Salmanvandi H & Ghaffarzadeh M, Soil, air, and water pollution from mining and industrial activities: Sources of pollution, environmental impacts, and prevention and control methods, *Results Eng*, 23 (2024) 102729.

8 Abanyie S K, Apea O B, Abagale S A, Amuah E E Y & Sunkari E D, Sources and factors influencing groundwater quality and associated health implications: A review, *Emerg Contam*, 9 (2023) 100207.

9 Saaristo M, Brodin T, Balshine S, Bertram M G, Brooks B W, Ehlman S M, McCallum E S, Sih A, Sundin J, Wong B B M & Arnold K E, Direct and indirect effects of chemical contaminants on the behaviour, ecology and evolution of wildlife, *Proc Royal Soc B*, 285 (2018) 20181297.

10 Mitra S, Saran R K, Srivastava S & Rensing C, Pesticides in the environment: Degradation routes, pesticide transformation products and ecotoxicological considerations, *Sci Total Environ*, 935 (2024) 173026.

11 Moradeeya P G, Sharma A, Kumar M A & Basha S, Titanium dioxide based nanocomposites-current trends and emerging strategies for the photocatalytic degradation of ruinous environmental pollutants, *Environ Res*, 204 (2022) 112384.

12 Saravanan A, Kumar P S, Vo D V N, Yaashikaa P R, Karishma S, Jeevanantham S, Gayatri B & Bharathi V D, Photocatalysis for removal of environmental pollutants and

fuel production: A review, *Environ Chem Lett*, 19 (2021) 441.

13 Al-Buriahi A K, Al-Gheethi A A, Kumar P S, Mohamed R M S R, Yusof H, Alshalif A F & Khalifa N A, Elimination of rhodamine B from textile wastewater using nanoparticle photocatalysts: A review for sustainable approaches, *Chemosphere*, 287 (2022) 132162.

14 Majumder S, Chatterjee S, Basnet P & Mukherjee J, ZnO based nanomaterials for photocatalytic degradation of aqueous pharmaceutical waste solutions-A contemporary review, *Environ Nanotechnol Monit Manage*, 14 (2020) 100386.

15 Marugan J, López-Muñoz M J, van Grieken R & Aguado J, Photocatalytic decolorization and mineralization of dyes with nanocrystalline TiO_2/SiO_2 materials, *Ind Eng Chem Res*, 46 (2007) 7605.

16 Wang S, Ding Z, Chang X, Xu J & Wang D H, Modified nano-TiO_2 based composites for environmental photocatalytic applications, *Catalysts*, 10 (2020) 759.

17 Chen J, Xiong Y, Duan M, Li X, Li J, Fang S, Qin S & Zhang R, Insight into the synergistic effect of adsorption–photocatalysis for the removal of organic dye pollutants by Cr-doped ZnO, *Langmuir*, 36 (2019) 520.

18 Fazal T, Razzaq A, Javed F, Hafeez A, Rashid N, Amjad U S, Faisal A U S, Rehman M S U, Faisal A & Rehman F, Integrating adsorption and photocatalysis: A cost effective strategy for textile wastewater treatment using hybrid biochar-TiO_2 composite, *J Hazard Mater*, 390 (2020) 121623.

19 Zhang L & Jaroniec M, Fundamentals of adsorption for photocatalysis, *Interface Sci Technol Interface Sci Technol*, 31 (2020) 39.

20 Wang T, Dissanayake P D, Sun M, Tao Z, Han W, An N, Gu Q, Xia D, Tian B, Ok Y S, & Shang J, Adsorption and visible-light photocatalytic degradation of organic pollutants by functionalized biochar: Role of iodine doping and reactive species, *Environ Res*, 197 (2021) 111026.

21 Liras M, Barawi M & de la Peña O'Shea V A, Hybrid materials based on conjugated polymers and inorganic semiconductors as photocatalysts: From environmental to energy applications, *Chem Soc Rev*, 48 (2019) 5454.

22 Amorim S M, Steffen G, de S Junior J M, Brusamarello C Z, Romio A P & Domenico M D, Synthesis, characterization, and application of polypyrrole/TiO_2 composites in photocatalytic processes: A review, *Polym Polym Compos*, 29 (2021) 1055.

23 Deng F, Min L, Luo X, Wu S & Luo S, Visible-light photocatalytic degradation performances and thermal stability due to the synergetic effect of TiO_2 with conductive copolymers of polyaniline and polypyrrole, *Nanoscale*, 5 (2013) 8703.

24 Silvestri S, Burgo T A, Dias-Ferreirak C, Labrincha J A & Tobaldi D M, Polypyrrole-TiO_2 composite for removal of 4-chlorophenol and diclofenac, *React Funct Polym*, 146 (2020) 104401.

25 Iqbal S & Ahmad S, Recent development in hybrid conducting polymers: Synthesis, applications and future prospects, *J Ind Eng Chem*, 60 (2018) 53.

26 Tan Y & Ghandi K, Kinetics and mechanism of pyrrole chemical polymerization, *Synth Met*, 175 (2013) 183.

27 Gao F, Hou X, Wang A, Chu G, Wu W J & Chen H Z, Preparation of polypyrrole/TiO_2 nanocomposites with enhanced photocatalytic performance, *Particuology*, 26 (2016) 73.

28 Sangareswari M & Sundaram M M, Development of efficiency improved polymer-modified TiO_2 for the photocatalytic degradation of an organic dye from wastewater environment, *Appl Water Sci*, 7 (2017) 1781.

29 Sun L, Shi Y, Li B, Li X & Wang Y, Preparation and characterization of polypyrrole/TiO_2 nanocomposites by reverse microemulsion polymerization and its photocatalytic activity for the degradation of methyl orange under natural light, *Polym Compos*, 34 (2013) 1076.

30 Li S, Xu S, He L, Xu F, Wang Y & Zhang L, Photocatalytic degradation of polyethylene plastic with polypyrrole/TiO_2 nanocomposite as photocatalyst, *Polym Plast Technol Eng*, 49 (2010) 400.

31 Villora-Picó J J, Belda-Alcázar V, García-Fernández M J, Serrano E, Sepúlveda-Escribano A & Pastor-Blas M M, Conducting polymer–TiO_2 hybrid materials: Application in the removal of nitrates from water, *Langmuir*, 35 (2019) 6089.

32 Moradeeya P G, Kumar M A, Sharma A & Basha S, Conductive polymer layered semiconductor for degradation of triclopyr acid and 2, 4-dichlorophenoxyacetic acid from aqueous stream using coalesce adsorption-photocatalysis technique, *Chemosphere*, 298 (2022) 134360.

33 Chen J, Shu C, Wang N, Feng J, Ma H & Yan W, Adsorbent synthesis of polypyrrole/TiO_2 for effective fluoride removal from aqueous solution for drinking water purification: Adsorbent characterization and adsorption mechanism, *J Colloid Interf Sci*, 495 (2017) 44.

34 Abramović B, Šojić D, Despotović V, Vione D, Pazzi M & Csanádi, A comparative study of the activity of TiO_2 Wackherr and Degussa P25 in the photocatalytic degradation of picloram, *J Appl Catal B*, 105 (2011) 191.

35 Arlos M J, Liang R, Fong L C L C, Zhou N Y, Ptacek C J, Andrews S A & Servos M R, Influence of methanol when used as a water-miscible carrier of pharmaceuticals in TiO_2 photocatalytic degradation experiments, *J Environ Chem Eng*, 5 (2017) 4497.

36 Zhang W, Zhang Y, Yang K, Yang Y, Jia J & Guo L, Photocatalytic performance of SiO_2/CNOs/TiO_2 to accelerate the degradation of Rhodamine B under visible light, *Nanomaterials*, 9 (2019) 1671.

37 Kite S V, Sathe D J, Patil S S, Bhosale P N & Garadkar K M, Nanostructured TiO_2 thin films by chemical bath deposition method for high photo electrochemical performance, *Mater Res Exp*, 6 (2018) 026411.

38 Lin W D, Chang H M & Wu R J, Applied novel sensing material graphene/polypyrrole for humidity sensor, *Sensors Actuat B Chem*, 18 (2013) 326.

39 Mahlake T, Tichapondwa S M, Tshuto T T & Chirwa E, The effect of crystalline phase on the simultaneous degradation of phenol and reduction of chromium (VI) using UV/TiO_2 photocatalysis, *Chem Eng Trans*, 76 (2019) 1279.

40 Li W, Liang R, Hu A, Huang Z & Zhou Y N, Generation of oxygen vacancies in visible light activated one-dimensional iodine TiO_2 photocatalysts, *RSC Adv*, 4 (2014) 36959.

41 Villabona-Leal E G, Escobar-Villanueva A G, Ovando-Medina V M, Pérez-Pérez E B, Díaz-Flores P E, Romero-Galarza A & Marquez-Herrera A, Semiconducting polypyrrole@ TiO_2 pure anatase nanoparticles for

photodegradation of reactive red 120 azo dye, *J Mater Sci Mater Electron*, 31 (2020) 12178.
42 Luo Q, Li X, Wang D, Wang Y & J An, Photocatalytic activity of polypyrrole/TiO_2 nanocomposites under visible and UV light, *J Mater Sci*, 46 (2011) 1646.
43 Al-Ghouti M A & Da'ana D A, Guidelines for the use and interpretation of adsorption isotherm models: A review, *J Hazard Mater*, 393 (2020) 122383.
44 Moradeeya P G, Kumar M A, Thorat R B, Rathod M, Khambhaty Y & Basha S, Nanocellulose for biosorption of chlorpyrifos from water: Chemometric optimization, kinetics and equilibrium, *Cellulose*, 24 (2017) 1319.
45 Debnath S, Ballav N, Maity A & Pillay K, Development of a polyaniline-lignocellulose composite for optimal adsorption of Congo red, *Int J Biol Macromol*, 75 (2015) 199.
46 Nama M, Satasiya G, Sahoo T P, Moradeeya P G, Sadukha S, Singhal K, Saravaia H T , Dineshkumar R & Kumar M A, Thermo-chemical behaviour of Dunaliellasalina biomass and valorising their biochar for naphthalene removal from aqueous rural environment, *Chemosphere*, 353 (2024) 141639.
47 Sahoo T P, Satasiya G, Moradeeya P G, Saravaia H T & Kumar M A, Removal of fluoroquinolone antibiotic and sulfonated dye by functionalized Persea americana seed powder: Appraisal on phase transfer kinetics, equilibrium, economics, and applications in rural settings, *Environ Res*, 261 (2024) 119727.
48 Wang J & Guo X, Adsorption kinetic models: Physical meanings, applications, and solving methods, *J Hazard Mater*, 390 (2020*)* 122156.
49 Wang J & Guo X, Adsorption kinetics and isotherm models of heavy metals by various adsorbents: An overview, *Crit Rev Environ Sci Technol*, 53 (2023) 1837.
50 Li J, Feng J & Yan W, Excellent adsorption and desorption characteristics of polypyrrole/TiO_2 composite for Methylene Blue, *Appl Surf Sci*, 279 (2013) 400.
51 Stejskal J, Trchová M, Bober P, Morávková Z, Kopecký D, Vrňata M & Watzlová E, Polypyrrole salts and bases: Superior conductivity of nanotubes and their stability towards the loss of conductivity by deprotonation, *RSC Adv*, 6 (2016) 88382.
52 Zhang P, Hong R Y, Chen Q & Feng W G, On the electrical conductivity and photocatalytic activity of aluminum-doped zinc oxide, *Powder Technol*, 253 (2014) 360.
53 Sun W, Chen L, Sun Y, Su Q, Wang Y & Liu J, The functional polypyrrole composite: A class of high-performing Cr(VI) ion adsorbents, *J Porous Mater*, 24 (2017) 519.
54 Khan M M, Khan A, Bhatti H N, Zahid M, Alissa S A, El-Badry Y A & Iqbal M, Composite of polypyrrole with sugarcane bagasse cellulosic biomass and adsorption efficiency for 2, 4-dicholrophonxy acetic acid in column mode, *J Mater Res Technol*, 15 (2021) 2016.
55 Sambaza S S, Maity A & Pillay K, Polyaniline-coated TiO_2 nanorods for photocatalytic degradation of bisphenol A in water, *ACS Omega*, 5 (2020) 29642.
56 Malato S, Fernández-Ibáñez P, Maldonado M I, Blanco J & Gernjak W, Decontamination and disinfection of water by solar photocatalysis: Recent overview and trends, *Catal Today*, 147 (2009) 1.
57 Behnajady M A, Mansoriieh N, Modirshahla N & Shokri M, Influence of operational parameters and kinetics analysis on the photocatalytic reduction of Cr (VI) by immobilized ZnO, *Environ Technol*, 33 (2012) 265.
58 Ali I, Park S & Kim J O, Modeling the photocatalytic reactions of g-C_3N_4-TiO_2 nanocomposites in a recirculating semi-batch reactor, *J Alloys Compd*, 821 (2020) 153498.
59 Gelaw T B & Sarojini B K, Enhancing the performance and recyclability of polyaniline/TiO_2 hybrid nanocomposite by immobilizing with zein/hydroxyethyl cellulose composites for removal of anionic dyes, *Asian J Chem*, 33 (2021) 1253.
60 Li X, Wang D, Cheng G, Luo Q, An J & Wang Y, Preparation of polyaniline-modified TiO_2 nanoparticles and their photocatalytic activity under visible light illumination, *Appl Catal B*, 81 (2008) 267.
61 Rathod M Moradeeya P G, Haldar S & Basha S, Nanocellulose/TiO_2 composites: Preparation, characterization and application in the photocatalytic degradation of a Potential endocrine disruptor, mefenamic acid, in aqueous media, *Photochem Photobiol Sci*, 17 (2018) 1301.